RESEARCH ARTICLE

CNT-Type Dependent Cellular Adhesion on 3D-Printed Nanocomposite for Tissue Engineering

Adam A. Mieloch[1]*, Julia A. Semba[1,2], Jakub D. Rybka[1]*

[1]Center for Advanced Technology, Adam Mickiewicz University, Poznan, Poland
[2]Faculty of Biology, Adam Mickiewicz University, Poznan, Poland

Abstract: At present, one of the main limitations of three-dimensional (3D) bioprinting in tissue engineering stems from a scarcity of biomaterials tailored for specific applications. Widely used hydrogels offer an optimal printability and a suitable environment for cell growth; however, they lack the mechanical strength required for non-soft tissues, for example, cartilage, tendons, and meniscus. This work investigated the physicochemical, mechanical, and biological characteristics of a 3D-printed polycaprolactone (PCL) reinforced with multiwalled carbon nanotubes (MWCNT) and "bamboo-like" carbon nanotubes (BCNT) with the following w/w % concentrations: 0.005%, 0.01%, 0.02%, and 0.2%. The materials were analyzed with subsequent techniques: Scanning electron microscopy, nanoindentation, parallel plate rheometry, and differential scanning calorimetry. Biological evaluations were performed with normal human articular chondrocytes by confocal microscopy and proliferation assay. The study revealed that the carbon nanotubes (CNT) addition improved the rheological properties of the material by increasing the setting temperature. Moderate enhancement was observed in terms of mechanical properties. The most significant difference was noted in cell adhesion and proliferation. Pure PCL did not facilitate cell growth and mainly apoptotic cells were observed on its surface. The addition of 0.01% MWCNT resulted in enhanced adhesion and proliferation; however, the morphology of the cells remained spherical, signifying a suboptimal surface for proliferation. Interestingly, PCL reinforced with 0.02% BCNT displayed excellent facilitation of cellular adhesion and proliferation, which is uncharacteristic of pure PCL. In summary, this study investigated the potential of CNT-reinforced PCL for 3D bioprinting and tissue engineering, highlighting key physicochemical, mechanical, and biological aspects of this biomaterial.

Keywords: 3D bioprinting; Polycaprolactone; Carbon nanotubes; Tissue engineering nanocomposite

*Correspondence to: Jakub D. Rybka, Center for Advanced Technology, Adam Mickiewicz University, Poznan, Poland; jrybka@amu.edu.pl; Adam A. Mieloch, Center for Advanced Technology, Adam Mickiewicz University, Poznan, Poland; amieloch@amu.edu.pl

Received: December 7, 2021; **Accepted:** January 15, 2022; **Published Online:** March 29, 2022

Citation: Mieloch AA, Semba JA, Rybka JD, 2022, CNT-Type Dependent Cellular Adhesion on 3D-Printed Nanocomposite for Tissue Engineering. *Int J Bioprint,* 8(2):548. http://doi.org/10.18063/ijb.v8i2.548

1. Introduction

Polycaprolactone (PCL) is a semicrystalline biodegradable polyester with a melting temperature of ~60°C. It is FDA-approved for use in surgical implants and drug delivery devices and is widely studied for applications in tissue engineering and regenerative medicine[1]. Due to its low melting temperature and proven biocompatibility, it is the most commonly used thermoplastic polymer for three-dimensional (3D) bioprinting[2-5]. However, its mechanical and bioadhesive properties are suboptimal for non-soft tissue engineering and can be improved on by implementing additives. Carbon nanotubes (CNT) are an excellent additive candidate, supplementing both inadequacies of the PCL. Structurally, CNT can be viewed as sheets of graphene rolled into cylinders. There are several morphologically distinct forms of CNT, resulting in varying physicochemical properties. Nonetheless, CNT are one of the strongest materials in nature with Young's modulus on the order of 270 – 950 GPa and tensile strength of 11 – 63 GPa[6]. In terms of biocompatibility, they have been extensively studied for tailored biomaterial engineering of tissues such as cardiac tissue, neural tissue, bone, and cartilage[7-10]. In addition, a significant body of work regarding CNT-reinforced nanocomposites and their characteristics can be found in

the literature[11-13]. For the purpose of this study, two types of CNT were selected: "bamboo-like" CNT (BNCT) and multiwalled CNT (MWCNT). "Bamboo-like" CNT (BCNT) resemble the cup-in-cup structure characteristic of the bamboo stem, with a high presence of surface defects. This type of CNT is comparatively inexpensive as its imperfect morphology does not require stringent synthesis conditions. MWCNT are composed of multiple single-walled CNT with diminishing diameters, arranged concentrically. Due to the diminished quantity of structural defects in comparison to BCNT, MWNCT can be used for tissue engineering applications requiring electrical conductivity[14]. In recent years, a lot of research has been devoted to electrospun PCL/CNT nanocomposites for tissue engineering purposes, indicating a growing interest in biopolymers with CNT additives[15-19]. In regard to PCL/CNT composites, a staggering amount of variables, such as CNT aspect ratios, purity, defects, functionalizations, entanglement within a polymer matrix, and interfacial interactions reduce any predictive attempts of resulting properties to an educated guess. In addition, the potential cytotoxicity of a nanocomposite material depends on the biodegradation rate and subsequent gradual release of the nanofiller into the tissue environment. Therefore, despite a plethora of relevant research, a specific application-driven design of CNT-reinforced polymers still requires extensive laboratory work. This work aimed to evaluate mechanical and biological properties of PCL reinforced with BCNT and MWCNT from a 3D bioprinting and tissue engineering point of view.

2. Materials and methods

2.1. Materials

CNT were purchased from NanoLab Inc. (USA, MA). MWCNT have a purity >85%, diameter 10 – 30 nm, and length 5 – 20 μm. BCNT have a purity >85%, diameter 10 – 30 nm, and length 5 – 20 μm. PCL used in this work was in powder (~50 000 MW, Polysciences Europe GmbH). LIVE/DEAD Viability/Cytotoxicity Kit for mammalian cells (Invitrogen) was also used in this study.

2.2. Cell culture

Human knee articular chondrocytes (NHAC-kn, Cat No: CC-2550, LONZA) were cultured in DMEM/F12 with L-glutamine (Corning) supplemented with 10% fetal bovine serum (FBS), 50 μg/mL 2-phospho-L-ascorbic acid, 50 U/ml penicillin, and 50 μg/ml streptomycin at standard culture conditions. The medium was changed every 3 days. Cells were subcultured at 80 – 90% confluence with the TrypLE Express Enzyme (Gibco). Chondrocytes up to the ninth passage and with cell viability above 95% were used for cell experiments.

2.3. Material preparation

The PCL and CNT powders were mixed in 15 ml Falcon tubes by shaking until a visually homogeneous powder was obtained. Subsequently, the powder was placed on a glass Petri dish and heated on a magnetic stirrer until melting occurred. The melt was cooled down and folded several times to improve the homogeneity of the material. Finally, the melt was cut into pellet-like pieces, which were suitable for the thermoplastic printhead.

2.4. 3D printing

3D printing was performed with the Cellink BioX printer. In the process, the thermoplastic printhead was utilized. The 3D model of the grid was prepared by manual writing of a.gcode file. The printing was performed with the following parameters: printhead nozzle diameter, 0.4 mm; printhead temperature, 180°C; printing speed, 4 mm/s; and extrusion pressure, 510 kPa.

2.5. Nanoindentation

The nanoindentation study was performed on a G200 (Agilent) nanoindenter equipped with a DCM head. Each sample was subjected to 12 indentations of 2000 nm in-depth, with a Berkovich-type probe, at room temperature. Analyses were performed at 500 – 1800 nm depth. Due to the uneven topography of the surface, extreme results were excluded from further analysis.

2.6. Parallel plate rheometry

The rheology study was performed with the Discovery Hybrid HR20 Rheometer (TA instruments). A 20 mm aluminum parallel plate was used for the measurements. A temperature sweep analysis was performed in two ranges: 120 – 40°C and 50 – 80°C. For both ranges, the temp. step was set to 2°C, 1% strain, and angular frequency at 10 rad/s. The soak time was set to 30 s. A flow sweep analysis was performed at three temperatures: 180°C, 120°C, and 60°C. The range of shear rate was set from 1×10^{-3} 1/s to 500.0 1/s, at logarithmic step. Data were analyzed using TA Instruments TRIOS Software version 5.1.1.46572.

2.7. Differential scanning calorimetry (DSC)

DSC analysis was performed on a DSC 8500 apparatus (Perkin Elmer) in the temperature range of −90 – 180°C, with nitrogen flow (20 ml/min). The temperature change rate was set at 10°C/min. The thermal history of the raw material was erased before measurement. 3D-printed grids were not subjected to thermal history erasure.

2.8. LIVE/DEAD viability/cytotoxicity kit for mammalian cells

3D-printed grids were cut and sterilized by ultraviolet (UV) light (30 min on each side). This experiment was carried out on 24-well Ultra-Low Attachment plates (Corning) in three biological replications. The chondrocytes were seeded on the grids at a density of 2×10^4 cells per well. The culture medium was changed every three days. The assay was carried out after 2 weeks of culture under standard conditions. The final concentrations of calcein-AM and EthD-1 were 2 and 4 μM, respectively. The labeled cells were visualized under confocal microscopy (Olympus XI83).

2.9. Cell Titer-Glo 2.0 cell viability assay

To investigate the potential toxicity of the materials, 3D-printed PCL grids were cut and sterilized with UV light (30 min on each side). This experiment was carried out on 24-well plates in three biological replications. Chondrocytes were seeded at a density of 2×10^4 cells per well. Positive control was cells seeded without the grid. After 3 and 6 days, the CellTiter-Glo 2.0 cell viability assay was carried out according to the manufacturer's manual with slight modifications. Briefly, 500 μl of fresh medium was added to each well, equilibrated to room temperature, followed by the addition of the CellTiter reagent. The plates were mixed for 2 min and incubated for 10 min at room temperature. Then, 200 μl of the solution was transferred to 96-well opaque-walled plates in at least two technical repeats. The luminescence was recorded using the Infinite 200 PRO plate reader (TECAN).

2.10. Statistical analysis

Statistical analysis was performed using GraphPad Prism ver. 8.0.1.

3. Results

3.1. Scanning electron microscopy (SEM) imaging

SEM imaging of the printed constructs revealed that the addition of CNT, regardless of their type and concentration, resulted in a much smoother surface in comparison to the pure PCL (**Figure S1**). The initial assumption was that the decrease in surface roughness will result in diminished cell attachment.

3.2. Parallel plate rheometry

Rheological properties are crucial from the standpoint of 3D printing and polymer manufacturing. It also provides valuable insight into the supramolecular interactions present within a material. The materials were subjected to the temperature sweep in the 120 – 40°C range, followed by a 50 – 80°C range sweep. Subsequently, flow sweep analysis was performed at three temperatures: 180°C, 120°C, and 60°C. Exemplary results of a pure PCL are presented in **Figure 1**.

The rest can be found in Supplementary File (**Figures S2-S4**). From the temperature sweep analysis, a point of modulus cross-over was obtained. The modulus cross-over signifies a temperature at which a change of the dominant modulus occurs. If the storage modulus (G') dominates, a material presents more elastic (solid-like) behavior. Conversely, if the loss modulus (G'') dominates, the material presents a more viscous (liquid-like) behavior. From the flow sweep analysis, zero-rate viscosity was calculated. The results are presented in **Table 1.**

The addition of CNT resulted in elevated temperature of modulus cross-over during cooling, regardless of CNT type. The highest increase was observed for 0.2% addition of BCNT and 0.2% MWCNT: 6.3°C and 5.2°C increase, respectively, in comparison to pure PCL. The temperature of modulus cross-over during heating was not pronouncedly affected by CNT addition. These observations indicate that CNT influence the solidification of PCL, but not melting. This led us to the suspicion that CNT may affect the crystallization of PCL either by acting as nucleation centers or by facilitating heat transfer through the polymer. Such phenomena have been described previously[20-22]. Regarding zero-rate viscosity, 0.01% addition of BCNT and MWCNT increased the polymer's viscosity. Interestingly, at the highest concentrations, a decrease in zero-rate viscosity was observed instead. Congruous data were obtained for all three temperatures. This result could be attributed to a gradual shift in dominant interactions between the CNT and PCL chains. At 0.01%, PCL/CNT interactions may predominate over PCL/PCL and CNT/CNT. With increasing CNT concentrations, the balance shifts toward CNT/CNT interactions, resulting in a decrease in zero-rate viscosity. The best fit flow analysis of viscosity vs. strain curve confirmed the pseudoplastic behavior of all tested materials. In most cases, the Carreau-Yasuda model was attributed to the experimental data[23,24]. Regardless of CNT addition, all samples showed similarity in viscosity vs. strain curve (**Figure S4**). At 60°C, the Newtonian plateau persisted until the shear rate of c.a. 6 1/s, where the transition region occurred. Due to limitations of the apparatus, further measurements beyond this point were unattainable. At 120°C, a prolonged Newtonian plateau was observed, followed by a well-pronounced transition region starting at c.a. 25 1/s, and a precipitous drop in viscosity, signifying the power-law region. At 180°C, the Newtonian plateau extended to the shear viscosity of c.a. 100 1/s. The transition region and the power-law were, in general, more flattened in comparison to 120°C.

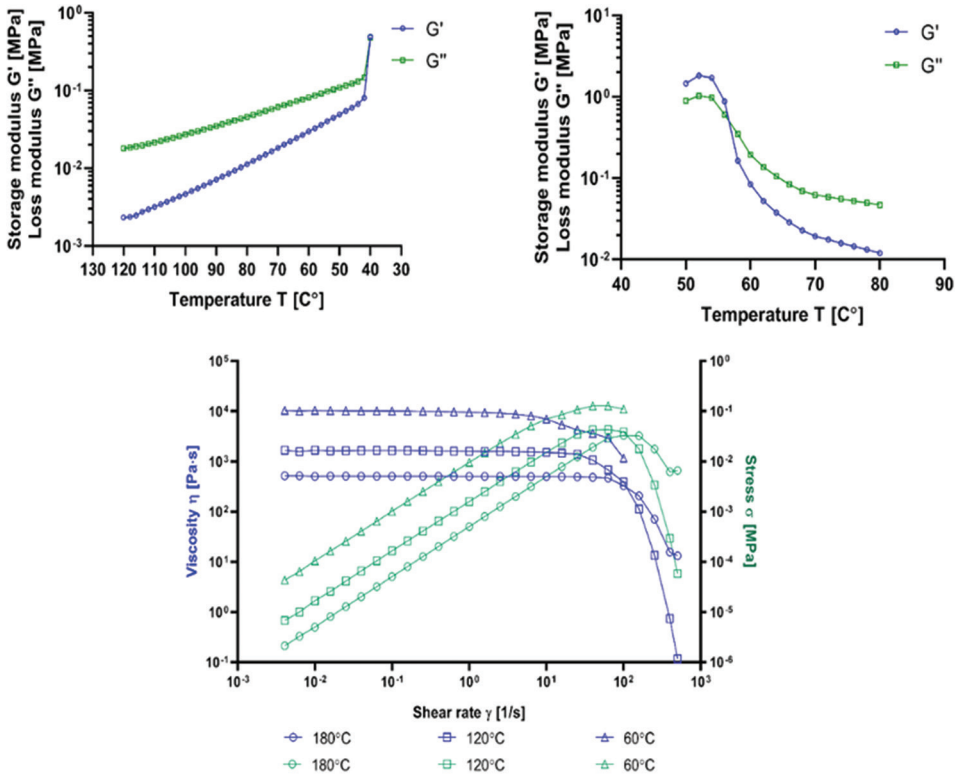

Figure 1. Example results of the temperature sweep and the flow sweep analysis (pure PCL).

Table 1. The modulus cross-over and zero-rate viscosity of the PCL at various CNTs concentrations.

	CNT content (w/w)	Modulus cross-over (°C)		Zero-rate viscosity (Pa·s)		
		120-40°C	50-80°C	180°C	120°C	60°C
PCL	0%	40.0	56.7	502.2	1579.6	10162.1
BCNT	0.005%	44.0	56.8	542.3	1662.8	10762.9
	0.01%	44.0	57.1	605.8	1892.9	10694.7
	0.02%	44.4	56.9	573.7	1775.7	9027.3
	0.2%	46.3	57.4	485.6	1536.2	7090.8
MWCNT	0.005%	42.8	57.0	555.4	1655.7	9729.2
	0.01%	42.6	56.9	579.7	1825.2	10252.4
	0.02%	44.0	57.1	569.8	1718.9	9377.6
	0.2%	45.2	57.2	452.6	1394.2	8445.1

In blue – minimum values; in red – maximum values. Zero-rate viscosity was calculated using best fit flow (viscosity vs. flow).

Obtained data indicates that the CNT addition does not affect the dynamics of shear-thinning behavior, displaying comparable viscosity versus strain curves across all samples at given temperatures. From this perspective, 120°C seems to be the most optimal for 3D printing of PCL, as it allows to fully utilize its shear-thinning behavior.

3.3. DSC

First, a DSC analysis was performed to assess the crystallinity of the raw material and the 3D 3D-printed grids. From the standpoint of a material investigation, it was vital to differentiate which factors affect crystallinity, namely, CNT addition or the 3D printing process. Therefore, the analysis of 3D printed grids was run without erasing the thermal history of the material, retaining its crystalline structure. The degree of crystallinity was calculated based on the heat of melting as:

$$\chi(\%) = \frac{\Delta H_m}{\Delta H_{m^0}} \cdot 100\%$$

where:

ΔH_m – the heat of melting (J/g)

$\Delta H_m{}^0$ – the heat of melting (J/g) for 100% crystalline polymer

The melting heat for 100% crystalline PCL is 139.5 J/g, which was adopted from the literature[25]. The results are summarized in **Table 2**.

The analysis revealed that the CNT addition does not affect substantially the overall crystallinity of the PCL. Interestingly, the process of 3D printing itself was much more influential, providing an 8.7% mean increase of crystallinity. Second, DSC analysis was utilized to investigate the crystallization dynamics of PCL + CNT blends. The rheological behavior of the samples suggests that the addition of CNT accelerates the solidification of the melts, which is associated with the crystallization of the material. The results confirmed the observations from the rheological analysis. The addition of CNT increases the temperature of crystallization onset (Tc) and the Tc (**Figure 2**). BCNT addition resulted in a mean increase of 4.0°C in the Tc onset and 6.9°C in the Tc. MWCNT addition provided a 2.9°C mean increase in the Tc onset and a 5.1°C mean increase in the Tc (**Table 3**). Despite not increasing overall crystallinity, CNT addition did enhance the crystallization rate of the PCL, calculated as Tc onset - Tc.

Table 2. The degree of crystallinity of the PCL at various CNTs concentrations.

	CNT content (w/w)	Degree of crystallinity (%)	
		Raw material	Grids
PCL	0%	50.75	59.00
BCNT	0.005%	51.38	59.94
	0.01%	50.68	60.20
	0.02%	50.14	60.26
	0.2%	50.91	61.92
MWCNT	0.005%	51.52	57.64
	0.01%	51.31	58.89
	0.02%	51.11	59.81
	0.2%	49.77	58.24

In blue – minimum values; in red – maximum values.

Table 3. The Tc and Tc onset the PCL at various CNTs concentrations.

	CNTs content (w/w)	Tc onset (°C)	Tc (°C)	Tc onset - Tc (°C)
PCL	0%	32.89	25.3	7.6
BCNT	0.005%	36.22	32.29	3.9
	0.01%	35.97	31.27	4.7
	0.02%	37.25	32.69	4.6
	0.2%	38.13	32.38	5.8
MWCNT	0.005%	33.66	27.93	5.7
	0.01%	35.43	29.65	5.8
	0.02%	36.54	31.91	4.6
	0.2%	37.62	32.01	5.6

In blue – minimum values; in red – maximum values.

3.4. Nanoindentation

Mean elastic modulus and mean hardness were measured via the nanoindentation method (**Figure 3**). Measurement was performed only on raw materials, as the curvature of 3D printed grids hinders reliable measurement. Therefore, we were unable to assess the effects of increased crystallinity on the mechanical properties of PCL reinforced with CNTs. The sole addition of CNTs did improve the mechanical properties of the material, however, in a nonlinear fashion. The highest increase in mean elastic modulus and hardness was observed for PCL with a concentration of 0.02% MWCNT.

3.5. LIVE/DEAD viability/cytotoxicity assay

Normal human knee articular chondrocytes (NHAC-kn) were seeded on the 3D printed grids and cultured for 2 weeks in standard conditions on non-adherent culture plates. After 2 weeks, cells were dyed with the LIVE/DEAD assay (**Figure 4**). The addition of CNTs did significantly affect the biocompatibility of the PCL. Chondrocytes seeded on pure PCL were mostly dead, while even the smallest concentration of 0.005% BCNT enhanced the viability. The enhancement was observed up to 0.02% concentration. At the highest tested concentration, BCNT decreased the viability of the chondrocytes in comparison to lower concentrations. The biocompatibility enhancement effect was less pronounced for PCL/MWCNT. A visible improvement was observed for the concentration of 0.01% MWCNT; however, it was still markedly worse compared to BCNT. Interestingly, BCNT addition facilitated a proper, elongated morphology of the chondrocytes, while this effect was absent in MWCNT-containing samples. In addition, the elongation occurred in parallel to the printhead movement, suggesting extrusion-driven topography alterations, dictating the direction of filopodia elongation. Cells on the PCL/MWCNT grids remained spherical and were rather loosely attached.

3.6. Cell Titer-Glo 2.0 cell viability assay

PCL is a biodegradable polymer; therefore, there is a risk of CNT-mediated cytotoxicity elicited by free-floating CNT, which are released from the polymer. To provide a quantitative analysis of cell viability, the CellTiter-Glo 2.0 Cell Viability assay was performed after three and 6 days of culture. In this experiment, cells were seeded on standard culture plates with inserted grids. After 3 days of culture, a slight increase of viability was observed for 0.01% MWCNT samples (**Figure 5**). On the other hand, 0.2% BCNT samples displayed markedly lower viability. As expected, the highest concentrations of CNT significantly decreased cell viability after 6 days of culture. Compared to control samples, 0.005 – 0.01%

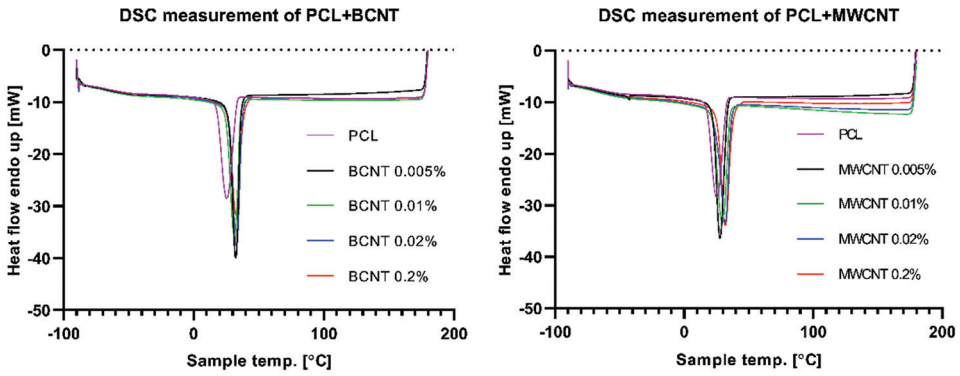

Figure 2. DSC measurement. Cooling step of raw materials (after thermal history erasure).

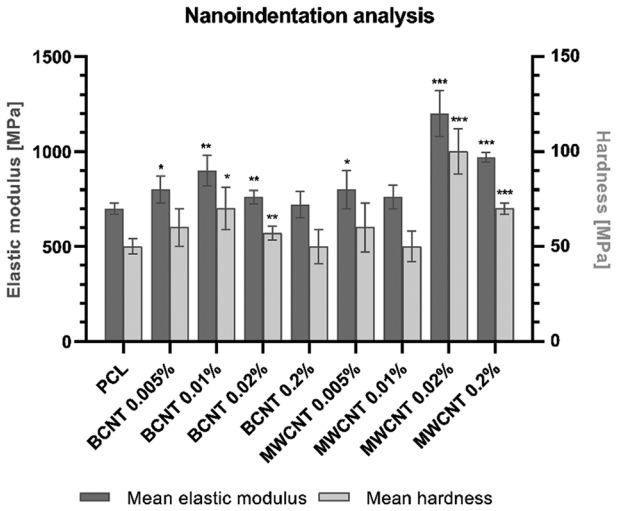

Figure 3. Mean elastic modulus and mean hardness of raw materials measured through nanoindentation. Statistical analysis was performed using one-way ANOVA and *post hoc* Dunnett's T3 multiple comparisons test. The mean of each column was compared to the mean of PCL column. CI = 95%, *P* value: 0.12 (ns), 0.033(*), 0.002 (**), <0.001 (***).

concentration range of both CNT types provided no statistically significant differences in viability. Pure PCL grids did have a minor effect on cell viability. The statistical significance of differences between samples against pure PCL was presented in the Supplementary File (**Table S1**).

4. Discussion

The data presented highlights several physicochemical, mechanical, and biological characteristics of PCL reinforced with CNT for 3D printing and tissue engineering. It is important to underline that the polymer mixing methodology most likely resulted in nonhomogeneous CNT dispersions within the polymer matrix, contributing to various characteristics of the resulting biomaterial. For an extensive overview of CNT/polymer nanocomposites and their interfacial characteristics, see the following article[26]. In our study, the addition of CNT resulted in a smoothened surface of the 3D-printed grids in comparison to pure PCL. As the data suggest, this effect cannot be explained by changes in viscosity or crystallinity of the samples. It could, however, be a result of an increased rate of crystallization, calculated as Tc onset - Tc. Presumably, CNT facilitate heat transfer through the polymer providing uniform temperature distribution, preventing local tensions arising from a nonequal rate of crystallization due to regional temperature differences. Contrary to this hypothesis, low concentrations of a thermoconductive filler are believed to facilitate phonons scattering at the filler/polymer interfaces, resulting in the "interface thermal resistance" phenomenon[27,28]. At this point, the mechanism of surface smoothening remains unsettled. However, taking into consideration the increase of the modulus cross-over temperature, Tc and Tc onset, with concomitant lack of increased overall crystallinity for CNT-reinforced PCL, supports the notion of enhanced thermal transfer.

Rheology analysis provided insight into the properties of the CNT/polymer interface. The initial increase of zero-rate viscosity at low to medium concentrations of CNT suggests that the strength of polymer/polymer interface interactions is lower than the polymer/CNT. However, at high CNT concentrations, zero-rate viscosity decreased below pure PCL, signifying the CNT/CNT interface being weaker in comparison to the polymer/polymer interface. Furthermore, the lack of increased viscosity at lower shear rates indicates that the CNT-filled PCL does not behave like a yield stress fluid (represented by the Herschel-Bulkley model)[29]. Therefore, it can be concluded that the CNT do not form cross-linked networks with the polymer chains. Moreover, it suggests that CNT do not act as nucleation centers for PCL crystallization, as was demonstrated for other polymers[30-32]. This finding is corroborated by the DSC data, revealing that the degree of crystallinity was not significantly affected by the CNT addition. Interestingly,

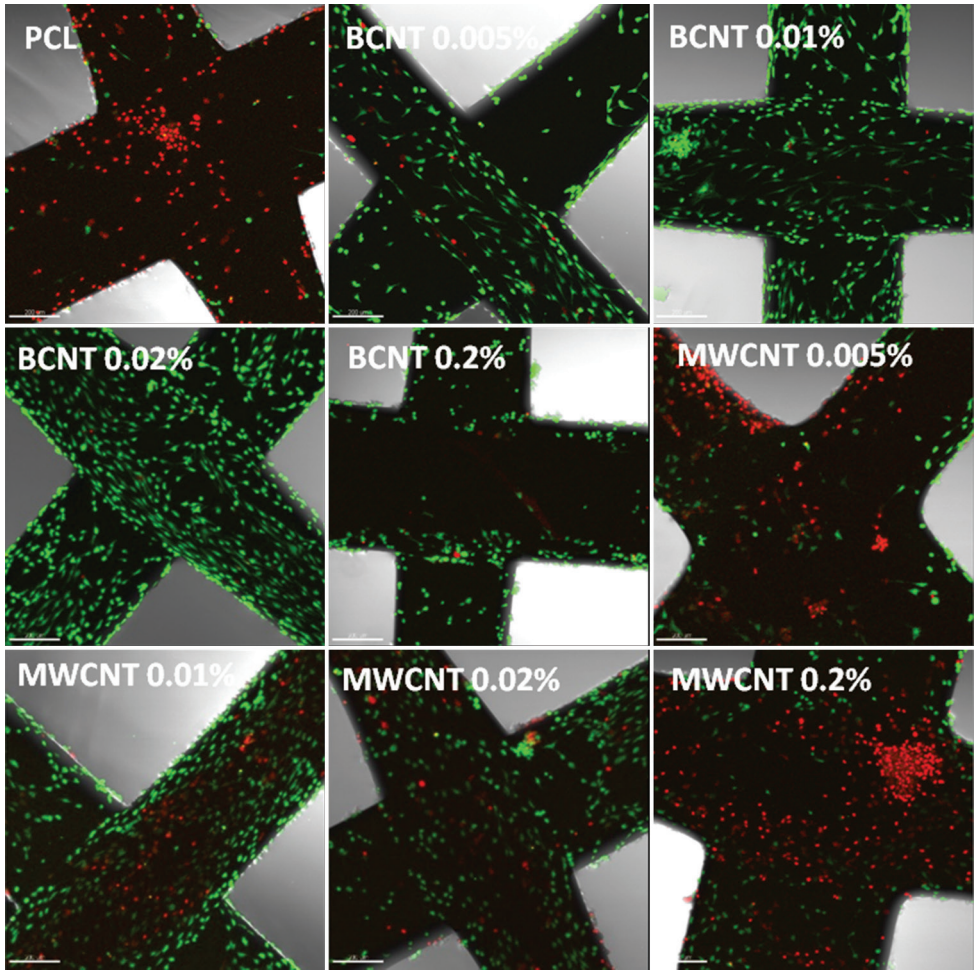

Figure 4. Confocal microscopy of LIVE/DEAD assay. Normal human knee articular chondrocytes (NHAC-kn) cultured for 2 weeks in standard conditions. Scale bars represent 200 μm.

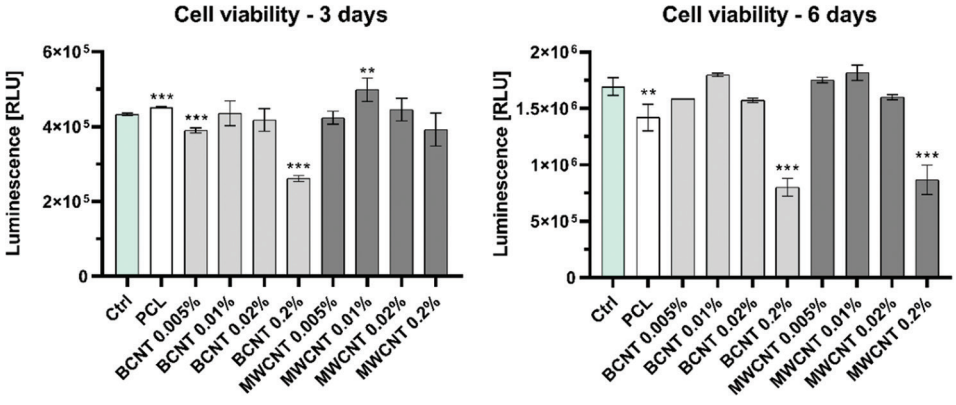

Figure 5. CellTiter-Glo 2.0 cell viability assay. Statistical analysis was performed using one-way ANOVA and *post hoc* Dunnett's T3 multiple comparisons test. The mean of each column was compared to the mean of the control (Ctrl) column. CI = 95%, *P* value: 0.12 (ns), 0.033(*), 0.002 (**), <0.001 (***).

the 3D printing process itself resulted in a significantly increased crystallinity compared to the raw material.

Regarding the mechanical properties assessed by nanoindentation, the addition of CNT did increase the hardness and elastic modulus of the PCL. The effect was the most pronounced for high concentrations of MWCNT. As mentioned previously, the main limitation of the study was the inability to measure 3D-printed grids

due to the cylindrical shape of the sample, which was unsuitable for nanoindentation. This obstacle prevented the comparison between more crystalline 3D-printed grids and raw material. Another factor that has to be taken into consideration is the nonhomogeneous dispersion of the nanotubes, which may form clusters within the material, potentially affecting the measurement.

Biological assessment of the materials revealed an extraordinary improvement in human knee chondrocyte proliferation and viability after the addition of BCNT. At 0.02 w/w% BCNT concentration, cells displayed an optimal morphology and enhanced proliferation. Interestingly, MWCNT addition also enhanced proliferation in comparison to pure PCL; however, cell morphology remained spherical, signifying nonoptimal adhesion to the surface. We suspect two potential mechanisms responsible for the observed effect: (i) Alterations of the surface zeta potential; and (ii) CNT protrusion from the polymer matrix, providing additional anchoring for the cells. In addition, the 3D printing process forces the alignment of CNT along the principal axis of the polymer extrusion, which coincides with the direction of the chondrocytes' filopodia projection, supporting the latter hypothesis. Unfortunately, no direct cause of the enhanced adhesion/proliferation has been found.

As mentioned previously, PCL is a biodegradable polymer, which entails a risk of gradual release of a filler into the environment[33-35]. Our cell viability assay performed after six days of culture showed a significant decrease in cell viability for the highest concentrations of CNT. The rate of biodegradation is a crucial factor, especially for potentially cytotoxic fillers. In theory, however, this could be mitigated by rapid extracellular matrix production, counteracting PCL degradation, and subsequently preventing CNT from being released into the environment.

5. Conclusions

Our study evaluated BCNT and MWCNT as fillers for PCL nanocomposites, dedicated for 3D bioprinting and tissue engineering. The following summary statements could be derived from this study: (i) CNT decreases the roughness of the 3D-printed constructs; (ii) CNT increases the temperature of modulus crossover, Tc, and Tc onset; (iii) the degree of crystallinity depends on the process of 3D printing rather than the CNT addition; (iv) BCNT addition favors cell growth and proliferation of human chondrocytes, facilitating their natural morphology; and (v) at high concentrations, CNT elicit cytotoxic effect and render the material rather unsuitable for tissue engineering purposes. In summary, this work provides novel aspects of PCL-based nanocomposites reinforced with CNT for 3D printing and tissue engineering.

Acknowledgments

The authors would like to thank Itedale Namro Redwan, Volodymyr Kuzmenko and Micheal Giersig for scientific support. Open access was cofounded by Excellence Initiative - Research University program, Call No. 040 "Open Access," grant 040/08/POB2/0001.

Funding

This work was supported by the National Center for Research and Development TECHMATSTRATEG-III/0027/2019-00 the National Science Centre UMO-2016/23/B/NZ7/01288 grants.

Conflict of interest

The authors declare no competing interests.

Author contributions

J.D.R. guided and supervised the project. A. A. M. designed and supervised the experiments. A. A. M., J.A.S., and J.D.R. conducted experiments and contributed intellectually to the scientific design of the project. A.A.M. and J.D.R. mentored the technical part of the project; manuscript preparation A.A.M and J.A.S.; manuscript edition J.D.R.

References

1. Li L, LaBarbera DV, 2017, 3D High-Content Screening of Organoids for Drug Discovery. In: Comprehensive Medicinal Chemistry III. Vol. 2-8. Amsterdam, Netherlands: Elsevier, p388–415.
2. Ramasamy S, Davoodi P, Vijayavenkataraman S, *et al*., 2021, Optimized Construction of a Full Thickness Human Skin Equivalent using 3D Bioprinting and a PCL/Collagen Dermal Scaffold. *Bioprinting*, 21:e00123. https://doi.org/10.1016/j.bprint.2020.e00123
3. Hassanajili S, Karami-Pour A, Oryan A, *et al*., 2019, Preparation and Characterization of PLA/PCL/HA Composite Scaffolds Using Indirect 3D Printing for Bone Tissue Engineering. *Mater Sci Eng C*, 104:109960. https://doi.org/10.1016/j.msec.2019.109960
4. Zhang W, Ullah I, Shi L, *et al*., 2019, Fabrication and Characterization of Porous Polycaprolactone Scaffold Via Extrusion-Based Cryogenic 3D Printing for Tissue Engineering. *Mater Des*, 180:107946. https://doi.org/10.1016/j.matdes.2019.107946
5. Duymaz BT, Erdiler FB, Alan T, *et al*., 2019, 3D Bio-Printing of Levan/Polycaprolactone/Gelatin Blends for Bone Tissue Engineering: Characterization of the Cellular Behavior. *Eur Polym J*, 119:426–37. https://doi.org/10.1016/j.eurpolymj.2019.08.015

6. Yu MF, Lourie O, Dyer MJ, *et al*., 2000, Strength and Breaking Mechanism of Multiwalled Carbon Nanotubes Under Tensile Load. *Science,* 287:637–40. https://doi.org/10.1126/science.287.5453.637
7. Szymański T, Mieloch AA, Richter M, *et al*., 2020, Utilization of Carbon Nanotubes in Manufacturing of 3D Cartilage and Bone Scaffolds. *Materials (Basel)*, 13:4039.
8. Patel DK, Dutta SD, Ganguly K, *et al*., 2021, Enhanced Osteogenic Potential of Unzipped Carbon Nanotubes for Tissue Engineering. *J Biomed Mater Res A*, 109:1869–80. https://doi.org/10.1002/jbm.a.37179
9. Edwards SL, Werkmeister JA, Ramshaw JA, 2009, Carbon Nanotubes in Scaffolds for Tissue Engineering. *Expert Rev Med. Dev*, 6:499–505.
10. Haniu H, Saito N, Matsuda Y, *et al*., 2012, Basic Potential of Carbon Nanotubes in Tissue Engineering Applications. *J Nanomater*, 2012:343747.
11. Soni SK, Thomas B, Kar VR, 2020, A Comprehensive Review on CNTs and CNT-Reinforced Composites: Syntheses, Characteristics and Applications. *Mater Today Commun*, 25:101546.
12. Stocco TD, Antonioli E, Romagnolli ML, *et al*., 2020, Aligned Biomimetic Scaffolds Based on Carbon Nanotubes-Reinforced Polymeric Nanofibers for Knee Meniscus Tissue *Eng Mater Lett*, 264:127351. https://doi.org/10.1016/j.matlet.2020.127351
13. Lebedev SM, 2020, PCL-CNT Nanocomposites Prepared by Melt Compounding and Evaluation of Their Basic Properties. *Polym Compos*, 41:1830–40. https://doi.org/10.1002/pc.25501
14. Abdal-Hay A, Taha M, Mousa HM, *et al*., 2019, Engineering of Electrically-Conductive Poly(E-Caprolactone)/Multi-Walled Carbon Nanotubes Composite Nanofibers for Tissue Engineering Applications. *Ceram Int*, 45:15736–40. https://doi.org/10.1016/j.ceramint.2019.04.206
15. Zadehnajar P, Akbari B, Karbasi S, *et al*., 2019, Preparation and Characterization of Poly ε-Caprolactone-Gelatin/Multi-Walled Carbon Nanotubes Electrospun Scaffolds for Cartilage Tissue Engineering Applications. *Int J Polym Mater Polym Biomater*, 69:326–37. https://doi.org/10.1080/00914037.2018.1563088
16. Jahanmard F, Eslaminejad MB, Amani-Tehran M, *et al*., 2020, Incorporation of F-MWCNTs into Electrospun Nanofibers Regulates Osteogenesis Through Stiffness and Nanotopography. *Mater Sci Eng C,* 106:110163. https://doi.org/10.1016/j.msec.2019.110163
17. Zadehnajar P, Karbasi S, Akbari B, *et al*., 2020, Incorporation of Multi-Walled Carbon Nanotubes Into Electrospun PCL/Gelatin Scaffold: The Influence on the Physical, Chemical and Thermal Properties and Cell Response for Tissue Engineering. *Mater Technol*, 35:39–49. https://doi.org/10.1080/10667857.2019.1651539
18. Wu T, Chen X, Sha J, *et al*., 2019, Fabrication of Shish-Kebab-Structured Carbon Nanotube/Poly(E-Caprolactone) Composite Nanofibers for Potential Tissue Engineering Applications. *Rare Met*, 38:64–72. https://doi.org/10.1007/s12598-017-0965-y
19. Zou Y, Zhang C, Wang P, *et al*., 2020, Electrospun Chitosan/Polycaprolactone Nanofibers Containing Chlorogenic Acid-Loaded Halloysite Nanotube for Active Food Packaging. *Carbohydr Polym*, 247:116711. https://doi.org/10.1016/j.carbpol.2020.116711
20. Yu W, Liu C, Fan S, 2021, Advances of CNT-Based Systems in Thermal Management. *Nano Res*, 14:2471–90.
21. Konstantopoulos G, Maroulas P, Dragatogiannis DA, *et al*., 2021, The Effect of Interfacial Resistance and Crystallinity on Heat Transfer Mechanism in Carbon Nanotube Reinforced Polyethylene. *Mater Des*, 199:109420. https://doi.org/10.1016/J.MATDES.2020.109420
22. Avramenko TG, Khutoryanskaya NV, Naumenko SM, *et al*., 2019, Effect of Carbon Nanofillers on Processes of Structural Relaxation in the Polymer Matrixes. In: Proceedings of the Springer Proceedings in Physics. Vol. 221. Cham: Springer, p293–305.
23. Carreau PJ, 1972, Rheological Equations from Molecular Network Theories. *Trans Soc Rheol,* 16:99–127. https://doi.org/10.1122/1.549276
24. Yasuda K, 1979, Investigation of the Analogies between Viscometric and Linear Viscoelastic Properties of Polystyrene Fluids, Massachusetts Institute of Technology.
25. Pitt CG, Chasalow FI, Hibionada YM, *et al*., 1981, Aliphatic Polyesters. I. The Degradation of Poly(ϵ-Caprolactone) *In Vivo*. *J Appl Polym Sci*, 26:3779–87. https://doi.org/10.1002/app.1981.070261124
26. Chen J, Liu B, Gao X, *et al*., 2018, A Review of the Interfacial Characteristics of Polymer Nanocomposites Containing Carbon Nanotubes. *RSC Adv*, 8:28048–85.
27. Evans W, Prasher R, Fish J, *et al*., 2008, Effect of Aggregation and Interfacial Thermal Resistance on Thermal Conductivity of Nanocomposites and Colloidal Nanofluids. *Int J Heat Mass Transf*, 51:1431–8. https://doi.org/10.1016/j.ijheatmasstransfer.2007.10.017
28. Klonos PA, Peoglos V, Bikiaris DN, *et al*., 2020, Rigid Amorphous Fraction and Thermal Diffusivity in

Nanocomposites Based on Poly(L-Lactic Acid) Filled with Carbon Nanotubes and Graphene Oxide. *J Phys Chem C*, 124:5469–79.
https://doi.org/10.1021/acs.jpcc.9b11843

29. Zhu H, Kim YD, de Kee D, 2005, Non-Newtonian Fluids with a Yield Stress. *J Nonnewton Fluid Mech*, 129:177–81.
https://doi.org/10.1016/j.jnnfm.2005.06.001
30. Wurm A, Herrmann A, Cornelius M, *et al*., 2015, TEMPERATURE dependency of Nucleation Efficiency of Carbon Nanotubes in Pet and PBT. *Macromol Mater Eng*, 300:637–49.
https://doi.org/10.1002/mame.201400405
31. Schawe JE, Pötschke P, Alig I, 2017, Nucleation Efficiency of Fillers in Polymer Crystallization Studied by Fast Scanning Calorimetry: Carbon Nanotubes in Polypropylene. *Polymer (Guildf)*, 116:160–72.
https://doi.org/10.1016/j.polymer.2017.03.072
32. Zhang S, Minus ML, Zhu L, *et al*., 2008, Polymer Transcrystallinity induced by Carbon Nanotubes. *Polymer (Guildf)*, 49:1356–64.
https://doi.org/10.1016/j.polymer.2008.01.018
33. Sun H, Mei L, Song C, *et al*., 2006, The *In Vivo* Degradation, Absorption and Excretion of PCL-Based Implant. *Biomaterials,* 27:1735–40.
https://doi.org/10.1016/j.biomaterials.2005.09.019
34. Goodwin DG, Boyer I, Devahif T, *et al*., 2018, Biodegradation of Carbon Nanotube/Polymer Nanocomposites Using a Monoculture. *Environ Sci Technol*, 52:40–51.
https://doi.org/10.1021/acs.est.7b02062
35. Frank BP, Goodwin DG, Bohutskyi P, *et al*., 2020, Influence of Polymer Type and Carbon Nanotube Properties on Carbon Nanotube/Polymer Nanocomposite Biodegradation. *Sci Total Environ*, 742:140642.
https://doi.org/10.1016/j.scitotenv.2020.140512

Publisher's note